EFFECTS OF MESOSCALE EDDIES ON SOUND CHANNELS

R Perks Atlas Elektronik UK
L Parkes Atlas Elektronik UK
I Siggers Atlas Elektronik UK

1 INTRODUCTION

The world's oceans have spatial and temporal variations in physical properties such as temperature and salinity. These properties are continually mixed through a variety of processes that act at a range of length and time scales, resulting in complex, turbulent mixing patterns. At mesoscales (typically 10-100s of kilometres) semi-stable patterns emerge which morph and evolve over periods of days, weeks and months. These patterns include the formation and evolution of ocean eddies. These phenomena are frequently generated at dynamic mixing locations, such as at western boundary currents or at frontal boundaries between water masses, where eddies are 'spun off' from the main jet. The resulting mesoscale eddies are dynamic, complex three-dimensional structures which exhibit different properties (such as temperature, salinity and vorticity) to their surrounding water. Since both temperature and salinity directly affect sound speed, the presence of an eddy has the potential to impact acoustic propagation.

The SOFAR (Sound Fixing and Ranging) channel is a naturally occurring sound channel in the oceans which was initially discovered by Ewing and Worzel in 1948[1] and subsequently investigated by various researchers. The depth of the SOFAR channel (i.e. its depth axis) is geographically dependant: in mid-latitudes depths of 1000-1200 m are common[2,3]; while in the Arctic summer depths as shallow as 100-200 m are reported[4]. Anthropogenic exploitation of this channel has included locating downed aviators (using a depth sensitive charge)[2] and long distance communication[5]. It is widely believed that marine mammals also exploit the channel for long range communication[6]. These include, large baleen whales (e.g. humpback, sperm) and elephant seals, which emit low frequency sound and have deep dive profiles[7].

A short study has been conducted to investigates how the presence of an eddy may affect acoustic propagation within such a sound channel.

2 METHODOLOGY

2.1 Overview

A simple, parameter-based, model was developed to represent ocean eddies. A variety of model representations were then embedded within a base ocean field. In each case, acoustic modelling was conducted to assess the impact that the eddy had on the acoustic propagation conditions.

2.2 Base Field

The base field was derived from a location close to the Bahamas[8] as shown by the star in Figure 1 left panel. In winter, this region contains a SOFAR channel at a depth of 1250 m as shown in Figure 1 right panel. This location has a sea floor depth of 4.4 km.

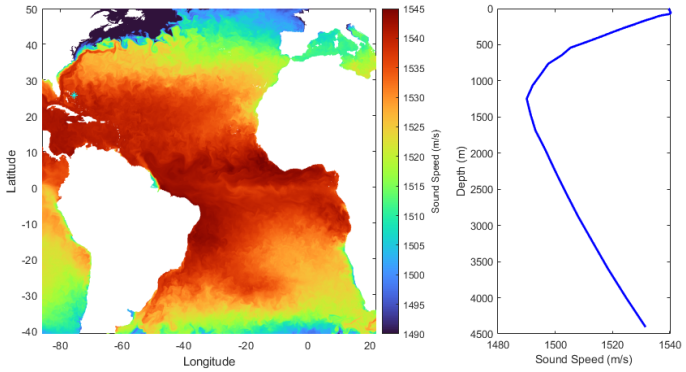

Figure 1: Sound speed at the ocean surface in the Atlantic in January (left). Sound speed profile (right) at the location of the star close to the Bahamas[9].

A horizontally invariant three dimensional field was generated by simply replicating this sound speed profile at all locations.

2.3 Modelling Eddies

A simple Gaussian distribution model (widely employed in the open literature[10, 11, 12] was used to represent eddies. A two dimensional deviation profile (in depth) was created, using Equation 1,

$$c(z) = c_{\pm} \times \delta c \times \exp\Big(-\Big(\frac{z - z_0}{\sqrt{2}\sigma}\Big)^2\Big), \tag{1}$$

where $c_{\pm}$ is equal to -1 or $+1$ depending on whether the eddy is a cold core or a warm core respectively, δc is the maximum sound speed deviation, z_0 is the depth of the centre of the eddy and σ is the standard deviation associated with Gaussian distributions, but here represents the vertical spread of the eddy. This two dimensional vertical profile represents the water column at the centre of the eddy. A three dimensional representation of the eddy was created using a Gaussian model for the lateral spread by applying Equation 2,

$$c(z, r) = c(z) \exp\Big(-\Big(\frac{r}{R}\Big)^2\Big), \tag{2}$$

where r is the radial distance from the centre of the eddy and R is the standard deviation of the lateral Gaussian model. Examples of a warm core and a cold core eddy are shown in Figure 2.

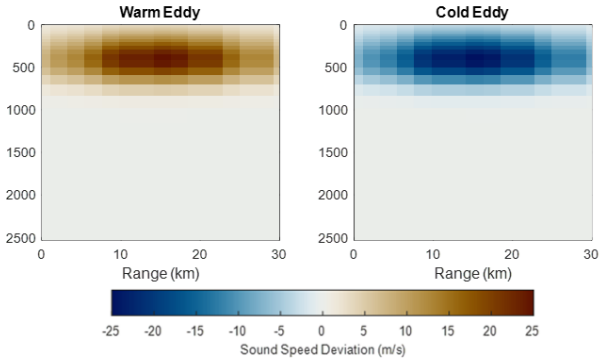

Figure 2: Sound speed deviation fields of a warm core (left) and a cold core (right) eddy.

2.4 Acoustic Analysis

Different physical environments were generated by combining the base field with the eddy deviation fields. In this paper three cases are considered: a No Eddy Case; a Warm Eddy Case; and a Cold Eddy Case. These three cases are depicted in Figure 3.

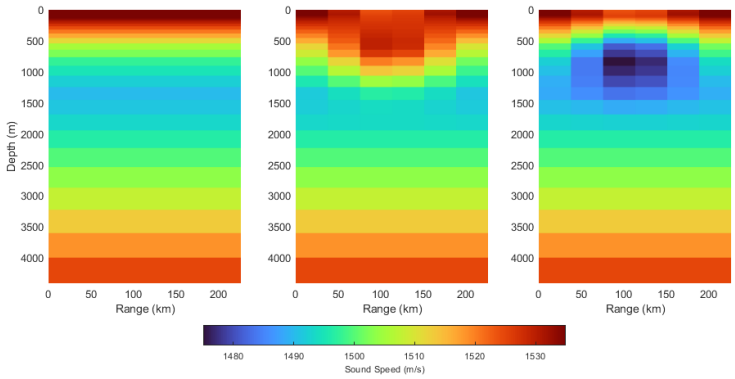

Figure 3: Sound speed plots for the No Eddy Case (left), the Warm Eddy Case (middle) and the Cold Eddy Case (right).

Acoustic modelling employed a two dimensional coherent parabolic equation model called SPUR which was derived from RAM (Range-dependent Acoustic Model)[13]. The model was run on 2 dimensional slices through the centre of the eddy, extending out to ranges of 250 km. The acoustic model was run at a frequency of 300 Hz. This frequency was chosen because it is low enough to avoid significant attenuation (at extended ranges) but is high enough to be affected by the presence of the eddy.

3 RESULTS

3.1 Scenario Parameters

The eddy parameters selected were:

- Eddy centre depth 600 m;
- Lateral extent 160 km; and
- Maximum sound speed deviation $\pm$ 25 m/s.

The edges of the eddy are located half the lateral extent (80 km) away from the centre of the eddy. The acoustic source was located at the depth of the eddy centre (600 m) and in two different lateral positions relative to the eddy.

- Scenario 1: 10 km from the edges of the eddy
- Scenario 2: At the centre of the eddy

3.2 Acoustic Analysis Results

Figure 4 shows the sound speed profile for the three cases. From this Figure the warm eddy causes the depth of the sound channel axis to increase (from 1.2 km to 1.5 km) whereas the cold eddy causes it to decrease (from 1.2 km to 0.75 km). In addition, the cold core eddy strengthens the sound channel by decreasing the minimum sound speed.

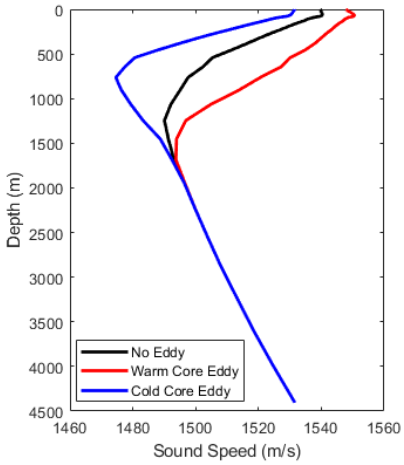

Figure 4: Sound speed profiles at the centre of the modelled eddy for warm core (red), cold core (blue) relative to the no eddy base field (black).

3.2.1 Ray Tracing

Figure 5 shows the variation in sound speed for the three cases within Scenario 1. In each Case the corresponding ray traces are overlaid, calculated from an Atlas Elektronik UK raytrace model which includes the effect of a range-dependent sound speed profile. The ray angles plotted are restricted to near-horizontal, $-5° : 0.5 : 5°$, to emphasise the sound channel's effect.

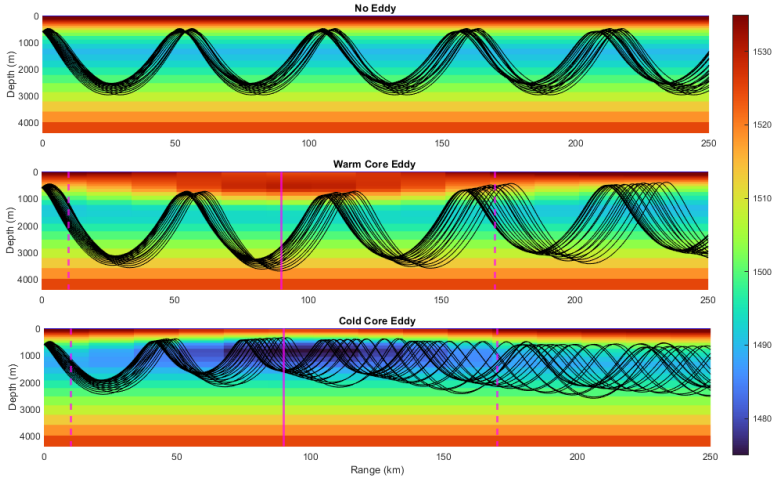

Figure 5: Sound speed variation and ray traces for the three cases in Scenario 1. The location of the eddy is marked in the upper two plots using a solid line for the centre and a dashed line for the edges.

A number of key observations from these plots are outlined below.

- In all three cases, the near-horizontal rays are trapped within the channel and do not interact with the boundaries.
- The Cold Eddy Case appears to have a greater impact on the ray paths than the Warm Eddy Case.

This is possibly because the depth of the sound source is co-located with the sound channel axis within the cold eddy.
- The depth extent of the rays, along with the rays amplitude, is increased in the Warm Eddy Case and decreased in the Cold Eddy Case.
- In the Warm Eddy Case, the ray divergence (as a function of range) in noticeably more pronounced than in the No Eddy Case. Ray divergence in the Cold Eddy Case is even more apparent.

Figure 6 shows the variation in sound speed for the three cases within Scenario 2 where the source is located at the centre (in both depth and range) of the eddy.

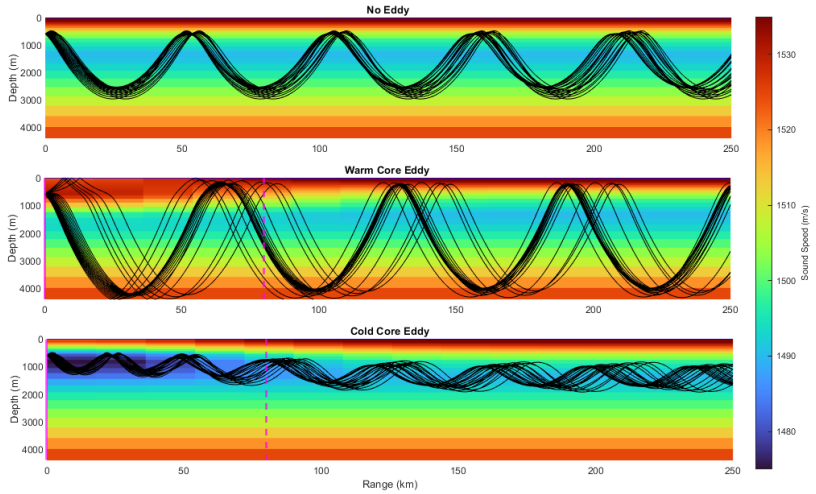

Figure 6: Sound speed variation and ray traces for the three cases in Scenario 2. The location of the eddy is marked in the upper two plots using a solid line for the centre and a dashed line for the edges.

The plots for this Scenario exhibit a number of key differences to Scenario 1 which are outlined below.

- In the Warm Eddy Case, the upward near-horizontal rays are refracted upwards and interact with the surface. The corresponding downward near-horizontal rays are refracted downwards and some of these interact with the sea floor. In this Case, the warm eddy diverges the rays away from the eddy centre (analogous to an optical concave lens).
- In the Cold Eddy Case, all the near-horizontal rays are tightly constrained within the channel. In this case, the cold core eddy converges the rays towards the eddy centre (analogous to an optical convex lens).

3.2.2 Propagation Loss

Figure 7 and Figure 8 shows the propagation loss (PL) for three cases within Scenario 1 and Scenario 2, respectively. These plots show where losses in acoustic energy are relatively high (dark blue) and relatively low (light blue through to yellow). In each Case the patterns observed are similar to the corresponding ray trace, shown in Figures 5 and 6. However, these propagation loss plots contain additional information and are not limited to near-horizontal launch angles. In the Warm Eddy Case in Scenario 2, the rays refracted up to the surface, or down to the sea bed, undergo high attenuation, so are less obvious in Figure 8 at larger ranges.

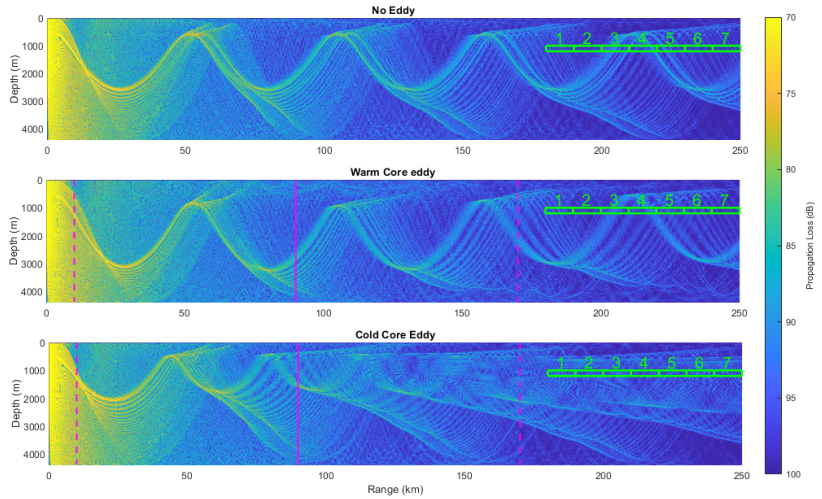

Figure 7: Propagation loss plotted as a function of range and depth for all cases in Scenario 1. The location of the eddy is marked in the upper two plots using a solid line for the centre and a dashed line for the edges. Regions analysed in further detail are highlighted in green.

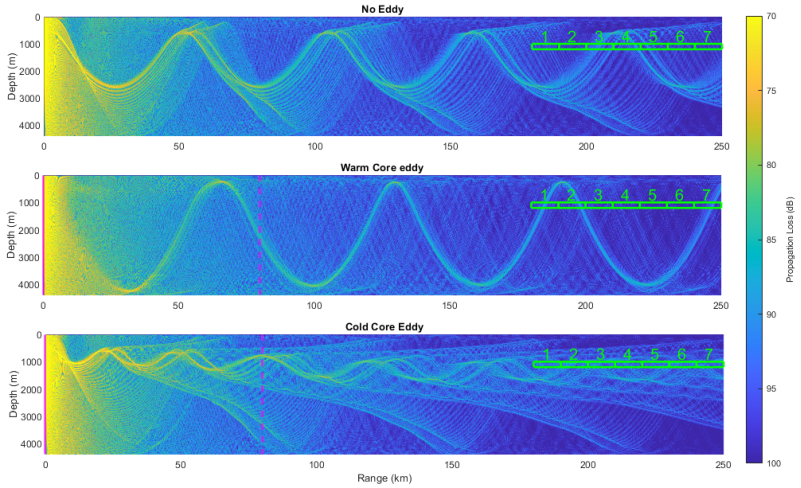

Figure 8: Propagation loss plotted as a function of range and depth for all cases in Scenario 2. The location of the eddy is marked in the upper two plots using a solid line for the centre and a dashed line for the edges. Regions analysed in further detail are highlighted in green.

Analysis was conducted on the PL values within the 10 km by 200 m green rectangles marked 1-7 on Figures 7 and 8. For both Scenarios and in all cases, the PL values were averaged over the green rectangles and the results are plotted in Figure 9. The location of these rectangles were selected for the reasons identified below.

- They lie outside the eddy and at the depth of the sound channel axis (at that location).
- The range extent (for 7 rectangles) is greater than a complete cycle (i.e. peak-to-peak distance) in all cases.

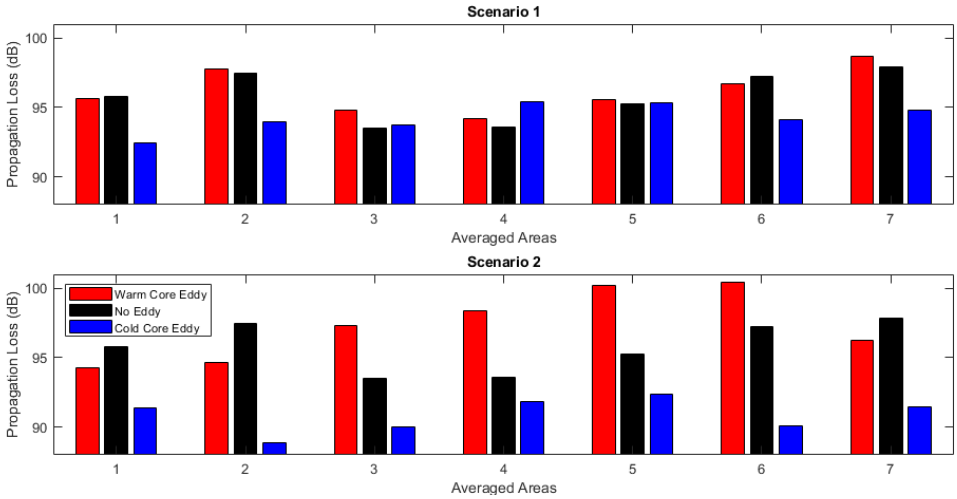

Figure 9: Averaged propagation loss for regions highlighted in Figures 7 and 8 for Scenario 1 (top) and Scenario 2 (bottom).

A number of key observations from Figures 7, 8 and 9 are outlined below.

- In Scenario 1, the Warm Eddy Case and No Eddy Case have similar averaged PL values across all 7 areas.
- Both Scenarios show a consistent cyclical trend in the Warm Eddy Case and No Eddy Case which is less apparent in the Cold Eddy Case.
- In Scenario 1, the Warm Eddy Case and No Eddy Case are in phase (following a similar cylindrical trend) whereas in Scenario 2 , the Warm Eddy Case and No Eddy Case appear to be out of phase.
- In Scenario 2 the Cold Eddy Case has consistently lower PL than the other two cases across all 7 areas.

4 CONCLUSIONS

The key findings from this paper are summarized below.

1. The Warm Eddy Case increased the depth of the sound channel axis whilst the Cold Eddy Case reduced the depth of the axis.
2. The Warm Eddy Case increased the depth extent of the sound channel whilst the Cold Eddy Case reduced it. This can be visualised by looking at the amplitude of the rays in each Case.
3. In the Cold Eddy Case the reduction of the depth of the sound channel axis moved it closer to the depth of the source. This re-positioned channel was narrow in depth. These various factors enhanced the propagation conditions.
4. In the Warm Eddy Case, with the source at the centre of the eddy, some near-horizontal rays are refracted up to the surface, or down to the sea bed, and undergo high attenuation. This means that less acoustic energy, emitted near the horizontal, enters the sound channel and propagates to extended ranges.
5. In the Cold Eddy Case divergence of the ray paths spread the acoustic energy whereas the energy in the Warm Eddy Case is largely contained within a single dominant path at extended ranges.

Based on this short study, a number of initial conclusions and recommendations have been identified.

1. This work indicates that the presence of an eddy can impact on acoustic propagation within a sound channel. Oceanographic understanding including knowledge of mesoscale eddies (i.e. their

disposition and structure), could potentially be exploited for acoustic purposes. For example, it may be beneficial to use the presence of an eddy to improve long distance communications. Also, this work could potentially have implications for underwater environmental assessment studies which need to consider the impact of acoustic noise on marine mammals.

2. For communications and transmission purposes, it may be advantageous to be located in a cold core eddy. To exploit this, the source would need to be within the eddy and the receiver located within the sound channel axis.
3. This work suggests that a cold core eddy may be more exploitable than a warm core eddy.
   (a) Based on key finding number 1, acoustic propagation employing a depth-constrained source located within, or close to, a cold core eddy could benefit from local shallowing of the sound channel.
   (b) Based on key finding number 5 with a source located within, or close to, a cold core eddy and a receiver located in the sound channel, the received level is relatively consistent with changing range separation. Whereas, in the Warm Eddy Case the received level is more sensitive to changing range separation.
4. Two key recommendations are outlined below.
   (a) Extend the modelling conducted within this study. This work should include varying the: base field; eddy parameters; and scenario geometry. This would underpin a more robust statistical evaluation of the acoustic impact of eddies on the sound channel.
   (b) Analysis of in-water measurements and ocean model outputs to validate the modelling approach and to inform the potential for future exploitation.

REFERENCES

1. M. Ewing and L.J. Worzel, "Long-range Sound Transmission" in *Geological Society of America Memoirs*, Geological Society of America, (1948), 1-32
2. J.R. Urick, *Principles of Underwater Sound*, 3, Maidenhead, England: McGraw Hill Higher Education, (1983)
3. K.F. Woolfe, S. Lane, K.G. Sabra and A.W. Kuperman, "Monitoring deep-ocean temperatures using acoustic ambient noise", *Geophys. Res. Lett.*, 42, 2878-2884, (2015)
4. L. Bjørnø and M.J. Buckingham, "General Characteristics of the Underwater Environment" in *Applied Underwater Acoustics*, Elsevier, (2017), 1-84
5. M. Stojanovic, "Underwater Acoustic Communications" in *Proceedings of Electro/International 1995*, IEEE, (2002)
6. R. Payne and D. Webb, "Orientation by Means of Long Range Acoustic Signaling in Baleen Whales", *Ann. N. Y. Acad. Sci.*, 188, 110-141, (1971)
7. M. André *et al.*, " Sperm Whale Long-range Echolocation Sounds Revealed by ANTARES, A Deep-sea Neutrino Telescope", *Sci. Rep.*, 114, 1266-1280, (2003)
8. S. C. Riser, H. Freeland, and H. T. Rossby, "Mesoscale motions near the deep western boundary of the North Atlantic," *Deep Sea Res.*, 25, 12, 1179–1191, (1978).
9. Global Ocean Physics Analysis and Forecast. E.U. Copernicus Marine Service Information (CMEMS). Marine Data Store (MDS). DOI: 10.48670/moi-00016 (Accessed on 12-2023).
10. J. Liu, S. Piao, L. Gong, M. Zhang, Y. Guo, and S. Zhang, "The effect of mesoscale eddy on the characteristic of sound propagation," *J. Mar. Sci. Eng.*, 9, 8, 787, (2021).
11. P. Gaube, D. B. Chelton, R. M. Samelson, M. G. Schlax, and L. W. O'Neill, "Satellite observations of mesoscale eddy-induced Ekman pumping," *J. Phys. Oceanogr.*, 45, 1, 104–132, (2015).
12. Z. Wang, Q. Li, L. Sun, S. Li, Y. Yang, and S. Liu, "The most typical shape of oceanic mesoscale eddies from global satellite sea level observations," *Front. Earth Sci.*, 9, 2, 202–208, (2015).
13. D. Miles, R. Hewitt, M. Donelly, T. Clarke and "Forward scattering of pulses from a rough sea surface by Fourier synthesis of parabolic equation solutions", *J. Acoust. Soc. Am.*, 114, 3, 1266-1280, (Sep 2003)